文章编号:1001-9014(2010)02-0081-06

WAVELENGTH EXTENDED InGaAs/InP PHOTODETECTOR STRUCTURES WITH LATTICE MISMATCH UP TO 2.6%

GU Yi[1], LI Cheng[1,2], WANG Kai[1,2], LI Hao-Si-Bai-Yin[1], LI Yao-Yao[1], ZHANG Yong-Gang[1]

(1. State Key Laboratory of Functional Materials for Informatics, Shanghai Institute of Microsystem and Information Technology, Chinese Academy of Sciences, Shanghai 200050, China;
2. Graduate School of Chinese Academy of Sciences, Beijing 100039, China)

Abstract: InP-based metamorphic InGaAs photodetector structures with lattice mismatch up to 2.6% were grown on InAlAs graded buffers with a relatively high mismatch grading rate of 1.1% μm^{-1} by gas source molecular beam epitaxy. They were compared to the samples with the same structures but smaller lattice mismatch of 1.7% and 2.1% to the InP substrate. Characteristics of the wafers were investigated by the measurements of atomic force microscopy, x-ray diffraction, photoluminescence and device performances. Results show that moderate surface morphology, large degree of relaxation and feasible optical characteristics have been obtained for the photodetector structures with lattice mismatch of 2.6%. The cut-off wavelength of the device is about 2.9μm at room temperature. The typical dark current of 2.56μA at room temperature has been achieved at reverse bias of 10 mV for the photodetector with 300 μm diameter.

Key words: photodetectors; buffer layer; InGaAs; lattice mismatch
CLC number: TN2 **Document**: A

晶格失配度达2.6%的波长扩展InGaAs/InP光电探测器结构

顾 溢[1], 李 成[1,2], 王 凯[1,2], 李好斯白音[1], 李耀耀[1], 张永刚[1]

(1. 中国科学院上海微系统与信息技术研究所 信息功能材料国家重点实验室, 上海 200050;
2. 中国科学院研究生院, 北京 100039)

摘要: 利用气态源分子束外延, 采用相对较高的1.1% μm^{-1}失配度变化速率, 在InAlAs递变缓冲层上生长了晶格失配度高达2.6%的InP基InGaAs变形晶格探测器结构, 并与采用相同结构而晶格失配度为1.7%和2.1%的探测器样品进行了比较。通过原子力显微镜、X射线衍射、光致发光和器件特性测试对样品进行了表征。结果显示该晶格失配度达2.6%的探测器结构具有较好的表面形貌、较大的晶格弛豫度和理想的光学特性。器件室温截止波长约为2.9μm, 直径为300μm的器件室温下在反向偏压10mV时的暗电流为2.56μA。

关 键 词: 光电探测器; 缓冲层; InGaAs; 晶格失配

Introduction

Photodetectors (PDs) with response wavelength of 1 ~ 3μm have many important applications, such as earth observation[1], special night vision[2], thermophotovoltaic for energy conversion[3], spectroscopy of characteristic absorption for gas detection[4], etc. In addition to HgCdTe and antimonide materials, the ternary InGaAs can also cover part of this wavelength range. For InGaAs, a relatively more mature growth and processing technology can be applied. Therefore, InGaAs PDs could be expected to have better perform-

Received date: 2009-08-15, **revised date**: 2009-12-28 **收稿日期**:2009-08-15, **修回日期**:2009-12-28
Foudantion item: Supported by the National Natural Science Foundation of China (No. 60876034) and 973 program (No. 2006CB604)
Biography: GU Yi, (1982-), male, Jiangsu, assistant researcher, research area is semiconductor optoelectronic materials and devices.

ances, especially at higher operation temperatures[5,6]. $In_{0.53}Ga_{0.47}As$ PDs lattice-matched to the InP substrate with cut-off wavelength of about 1.7μm have been widely used in fiber communication applications. The response can be shifted to longer wavelength by increasing the In content in the InGaAs alloy, whereas introducing a quite large lattice mismatch between InGaAs absorption layer and InP substrate. Wavelength extended InGaAs PDs grown by using hydride vapor phase epitaxy (HVPE)[5,6], metal organic chemical vapor deposition (MOCVD)[7,8] or molecular beam epitaxy (MBE)[9,10] with different cut-off wavelengths have been reported. Among these works, the cut-off wavelengths of the PDs are usually extended to shorter than 2.4μm, corresponding to a lattice mismatch of about 1.7% to the InP substrate. The reports about InGaAs PDs with lattice mismatch larger than 2.2% to the InP substrate have not been seen to our knowledge. In the wavelength extended PD structures, a suitable buffer layer between InP substrate and InGaAs absorption layer should be inserted to overcome the propagation of misfit dislocations and degradation of the material quality. The InAlAs continuously graded buffer grown by MBE technology is a feasible scheme for the metamorphic InGaAs PD structures as the convenient composition control in MBE[9,10], whereas a thin buffer should be preferable from a practical point of view as the growth rate of MBE is limited to around 1μm/h in practice.

In this paper, the characteristics of the MBE grown InP-based metamorphic InGaAs PD structure with up to 2.6% mismatch and the effects of the InAlAs continuously graded buffer with a relatively high grading rate of about 1.1% μm^{-1} have been reported. The metamorphic PD structures with 1.7% and 2.1% mismatch to the InP substrate with nearly the same grading rates were also grown and characterized as references.

1 Experimental details

The samples were grown on (100)-oriented InP epi-ready substrates by using a VG Semicon V80H gas source molecular beam epitaxy (GSMBE) system. The elemental In, Ga and Al sources were used as group III sources, and their fluxes were controlled by changing the cell temperatures. Arsine (AsH_3) and phosphine (PH_3) cracking cells were used as group V sources, and their fluxes were controlled by adjusting the pressure. The cracking temperature was around 1000 ℃. Standard Be and Si effusion cells were used as p-and n-type doping sources, and the doping levels were also controlled by changing the temperatures. Before growth, the fluxes of group III sources were calibrated by using an in situ ion gauge. The surface oxide desorption of the substrates was carried out under P_2 flux, including a slow ramp-up of the substrate temperature until the reflection high energy electron diffraction (RHEED) pattern showed an abrupt transformation to 2×4 surface reconstruction.

The epitaxy structures of the metamorphic PDs started from an N^+ $In_xAl_{1-x}As$ continuously graded buffer layer, and the In composition x was graded from 0.52 to a desired value y through the simultaneously linear increase of In source temperature and decrease of Al source temperature. After that, a 1.5μm n^- $In_yGa_{1-y}As$ absorption layer and a 0.6μm P^+ $In_yAl_{1-y}As$ cap layer were grown. The targeted cut-off wavelengths of the PDs were set to be 2.4μm, 2.7μm and 2.9μm for samples (a), (b), and (c), corresponding to the desired value y of around 0.78, 0.84, and 0.90, and lattice mismatch of about 1.7%, 2.1%, and 2.6% to the InP substrate, respectively. The thicknesses d of the $In_xAl_{1-x}As$ buffer layer were about 1.4μm, 2.0μm, and 2.4μm, corresponding to the lattice mismatch grading rates of buffer layers of about 1.2% μm^{-1}, 1.1% μm^{-1}, and 1.1% μm^{-1}, respectively. The growth rates of all layers were around 1μm/h.

After growth, the morphologies of the grown samples were observed by using an atomic force microscope (AFM). The $\omega/2\theta$ rocking curves and reciprocal space mappings (RSMs) were measured by using a Philips X'pert MRD high resolution x-ray diffractometer (HRXRD) equipped with a four-crystal Ge (220) monochromator. The PL spectra were measured by using a Nicolet Megna 860 Fourier transform infrared (FTIR) spectrometer, in which liquid-nitrogen cooled InSb detector and CaF_2 beam splitter were used. The samples were mounted onto a continuous-flow helium

cryostat to change the temperature, and a Coherent INNOVA 305 argon-ion laser (λ = 514.5nm) was used as an excitation source. The wafers were also processed into mesa-type PDs. The mesas were defined by using photolithography and wet etching, and then passivated by Si_3N_4 using plasma enhanced chemical vapor deposition (PECVD). After forming contact and alloy step, the wafers were diced into chips. A HP4156A precise semiconductor analyzer was used to perform the dark current measurements at room temperature. A Nicolet Magna 760 FTIR spectrometer was used to measure the response spectra. In the measurement CaF_2 beam splitter and Ever-Glo IR source were used.

2 Results and discussion

2.1 Atomic force microscope

The AFM images with 40 × 40μm² scan area are shown in Fig 1. A regular cross-hatch pattern exists for these lattice-mismatched PD structures. This type of pattern could be attributed to the two types of misfit dislocations A and B oriented along the [1$\bar{1}$0] and [110] directions, corresponding to group V and III atom-based cores, respectively[11]. Along the [1$\bar{1}$0] direction, the primary ridges are in parallel, and the periods of primary ridges are around 5μm, 6μm, and 8μm for samples (a), (b), and (c), respectively.

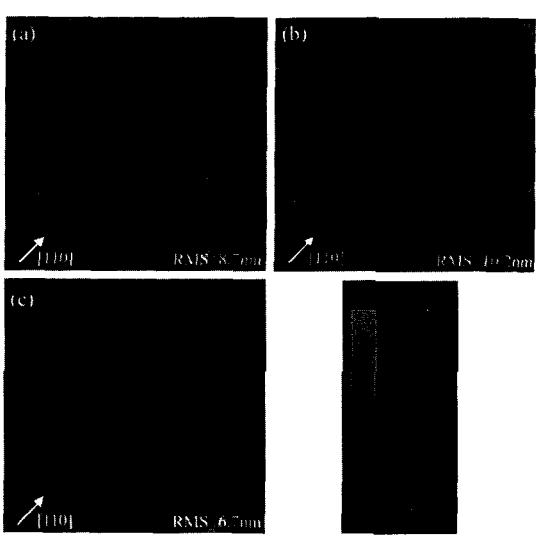

Fig. 1 AFM images of InGaAs PD structures with different lattice mismatch (a)1.7% (b)2.1% (c)2.6% (40 × 40μm²)
图 1 不同晶格失配 InGaAs 探测器结构的原子力显微镜图像 (a)1.7% (b)2.1% (c)2.6% (40 × 40μm²)

The period increases with the lattice mismatch. On the ridges small undulations exist periodically and the oval-like defects pop out on the top of the ridges. The period of the small undulations is around 1μm. The root mean square (RMS) roughness values are 8.7nm, 10.2nm and 6.7nm for samples (a), (b) and (c), respectively. For sample (c) with the largest epi-layer mismatch to the InP substrate, the oval-like defects seem more distinct. Nevertheless, the differences of morphologies for these three samples are not so obvious to distinguish the quality of the wafers, and the roughness values are all tolerable for further device processing.

2.2 X-ray diffraction

To characterize the structural properties of the samples, x-ray diffraction measurements were used. Fig. 2 shows the (004) $\omega/2\theta$ rocking curves of different samples and Table 1 lists the extracted results. There are a substrate peak and a layer peak in each rocking curve, where the relatively narrower peak corresponds to the substrate peak and the relatively broader peak to the layer peak. The layer peak is merged by the InAlAs cap layer and InGaAs absorption layer with almost same In composition. The In compositions of the epi-layers are around (a)0.77, (b)0.83 and (c)0.91 on average from full relaxation estimation, which are close to our targeted In compositions. With the increase of the In composition, the full width at half maximum (FWHM) is slightly broadened and the intensity of the layer peak is slightly decreased, which can be attributed to the degradation of the crystalline

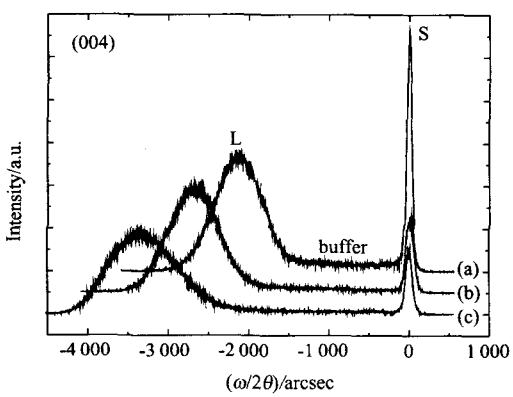

Fig. 2 HRXRD rocking curves of InGaAs PD structures with different lattice mismatch (a)1.7% (b)2.1% (c)2.6%
图 2 不同晶格失配 InGaAs 探测器结构的 HRXRD 摇摆曲线 (a)1.7% (b)2.1% (c)2.6%

表1 从HRXRD摇摆曲线提取的结果
Table 1 Results from HRXRD rocking curves

Sample	Buffer thickness/ Mismatch grading rates(μm)/ (%μm^{-1})	L peak intensity/ FWHM (arcsec)	Relaxed In composition	Relaxed lattice mismatch(%)
(a)	1.4/1.2	10807/680	0.772	1.67
(b)	2.0/1.1	9490/744	0.834	2.09
(c)	2.4/1.1	7206/1015	0.910	2.62

quality as expected. To judge whether the buffer layer is efficient for the metamorphic growth, it is necessary to investigate the relaxation status of the epi-layers, and the RSM measurements should be introduced.

The symmetric (004) and asymmetric (224) RSM reflections were measured and shown on the left and right sides of Fig. 3, respectively. The intensities are in the logarithmic scale. In all RSMs, the relatively narrow and circular peaks correspond to the InP substrate (denoted as S). The diffraction features from individual epitaxy layers are distinguished in the RSMs. The two layer peaks correspond to the InGaAs absorption layer (denoted as L1) and InAlAs cap layer (denoted as L2), respectively. They are elliptical with a larger diffuse scattering perpendicular to the normal line due to the existence of dislocations. L1 and L2 were assigned by measuring the HRXRD rocking curves in the same directions before and after etching the InAlAs cap layer. The layer peak was shifted toward the substrate side after the etching. On the (004) reflections, the divergencies of the centers of substrate peaks and layer peaks along the horizontal direction correspond to the macroscopic tilts of the layers to substrates[12]. The tilt angles of L1 to the substrate are −1.1°, 1.1°, and 1.1° for samples (a), (b) and (c), respectively. For the (224) reflections, the intensities of substrate peaks are weaker than those of layer peaks due to the thick epi-layers. The lines of full relaxation (metamorphic) and full pseudomorphic to the substrates were given on the (224) reflections for references. The contours of layers are all far from the pseudomorphic lines, indicating that the strain has been relaxed through the InAlAs graded buffer layers. The parallel mismatch $f_{//}$ and perpendicular mismatch $f_{\perp}$ of the InGaAs absorption layers were extracted from the RSMs, and then the cubic lattice mismatch f and

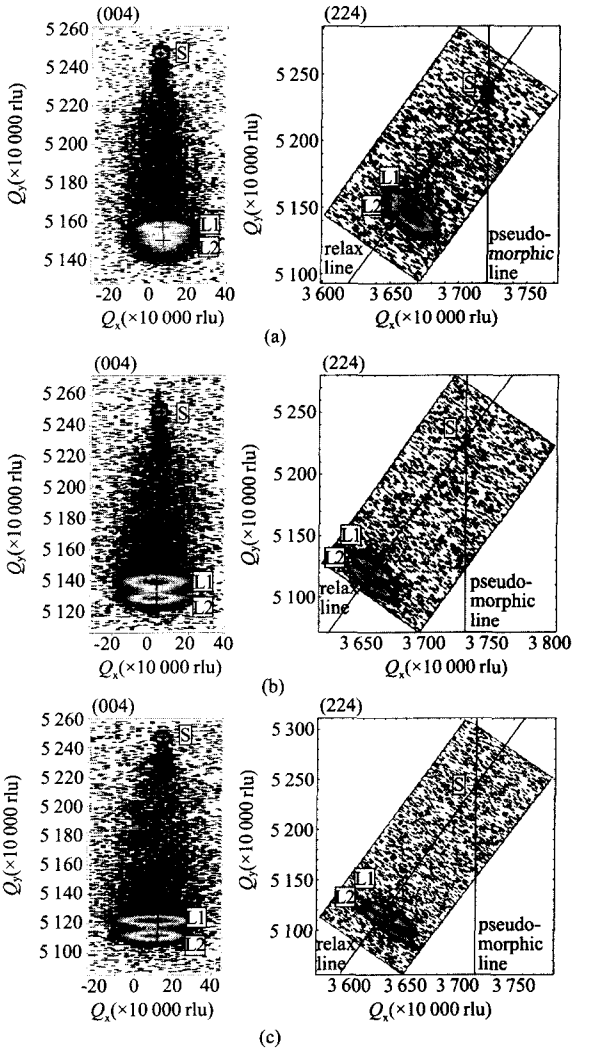

Fig. 3 HRXRD RSMs of InGaAs PD structures with different lattice mismatch (a)1.7% (b)2.1% (c)2.6%
图3 不同晶格失配InGaAs探测器结构的HRXRD RSM图 (a)1.7% (b)2.1% (c)2.6%

In composition y were calculated by the following equations[13]:

$$f = \left(\frac{1-v}{1+v}\right) f_{\perp} + \frac{2v}{1+v} f_{//} \quad , \tag{1}$$

$$f = \frac{y a_{\mathrm{InAs}} + (1-y) a_{\mathrm{GaAs}} - a_{\mathrm{InP}}}{a_{\mathrm{InP}}} \quad , \tag{2}$$

where a_{InAs}, a_{GaAs}, and a_{InP} are the lattice constants of InAs, GaAs, and InP, respectively. v is the Poisson coefficient of $In_yGa_{1-y}As$, and can be given by the elastic constants c_{11} and c_{12} as:

$$v = \frac{c_{12}}{c_{11} + c_{12}} \quad . \tag{3}$$

The values of c_{11} and c_{12} were linearly interpolated by the parameters of binary InAs and GaAs[14]. The de-

表 2　Results from HRXRD (224) RSM measurements
Table 2　从 HRXRD(224)面 RSM 测试提取的结果

Sample	Buffer thickness/ Mismatch grading rates(μm)/ (% μm^{-1})	L1 In composition y	L1 cubic mismatch f(%)	L1 degree of relaxation R(%)
(a)	1.4/1.2	0.773	1.68	92.6
(b)	2.0/1.1	0.833	2.09	97.1
(c)	2.4/1.1	0.870	2.38	92.4

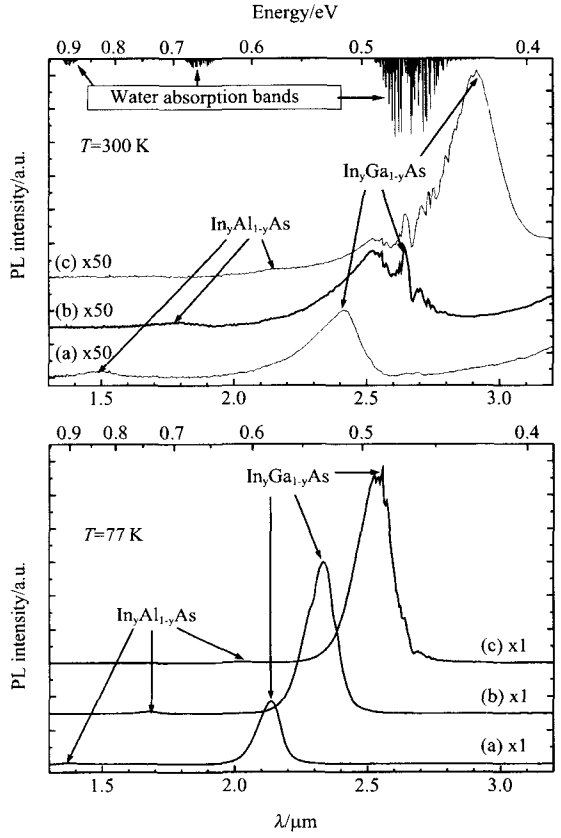

Fig. 4　PL spectra at 300 K and 77 K of InGaAs PD structures with different lattice mismatch, the water absorption bands are indicated for references
图 4　不同晶格失配 InGaAs 探测器结构的 300 K 和 77 K 下光致发光谱,图中也画出了水汽吸收带作为参考

grees of relaxation R for the InGaAs layers were then calculated from $R = f_{//}/f$ and listed in Table 2. For all the three samples, the degrees of relaxation are larger than 90%. Therefore, by using the InAlAs graded buffer layers with the grading rates of around 1.1% μm^{-1}, the InGaAs layers have been relaxed efficiently in all samples.

2.3　Photoluminescence

The optical properties of the epi-layers are most important in understanding the quality of the materials for optoelectronic applications. Fig. 4 shows the PL spectra of the samples at 300 K and 77 K. The centers of the spectral envelope of the PL signal are identified as the PL peaks and denoted in Fig. 4, noting that the water absorption bands have affected the PL signals, especially in the wavelength range of 2.5 ~ 2.8μm. The blue-shift of the PL envelops as the temperature decreases can help for the peak identification. Two PL envelops can be observed for every sample. The stronger one with the longer wavelength corresponds to the InGaAs absorption layer, and the weaker one with the shorter wavelength corresponds to the InAlAs cap layer. The centers of the PL envelops corresponding to the InGaAs absorption layers are at about 2.41 μm, 2.65 μm, and 2.91 μm at 300K, and blue-shift to 2.14 μm, 2.34 μm, and 2.54 μm at 77K, respectively, which are in agreement with the theoretical PL wavelengths from the In compositions. The PL intensities increase to about 50 times as the temperature decreases from 300 K to 77 K. An unexpected phenomenon is noticed that the PL intensity corresponding to the InGaAs layer of sample (c) with larger mismatch to the InP substrate is stronger than that of samples (a) and (b). The instrument function related to the response increase of InSb detector and CaF_2 beam splitter at longer wavelength may be the reason. Nevertheless, it is definite that favorable optical characteristics can be obtained for the InP-based PD structure with up to 2.6% mismatch by using InAlAs continuously graded buffer with the grading rate of about 1.1% μm^{-1}.

2.4　Device performances

To confirm the quality of the wafers, the dark current performances of the PDs were measured for the mesa-type devices with 300 μm diameter. Fig. 5 shows the I-V characteristics of the PDs. At reverse bias V_R = 10 mV, the dark currents are 0.426 μA (6.03×10^{-4} A/cm^2), 0.838μA (1.19×10^{-3} A/cm^2), and 2.56 μA (3.62×10^{-3} A/cm^2) for samples (a), (b), and (c), respectively. It is indicated that more nonradiative centers are generated for sample (c) due to more dislocations introduced by the larger lattice mismatch. Nevertheless, the dark current performance of sample (c) is even better than our previous results of the metamorphic PD with about 2.1% mismatch to the InP substrate and a grading rate of about 0.7% μm^{-1} for

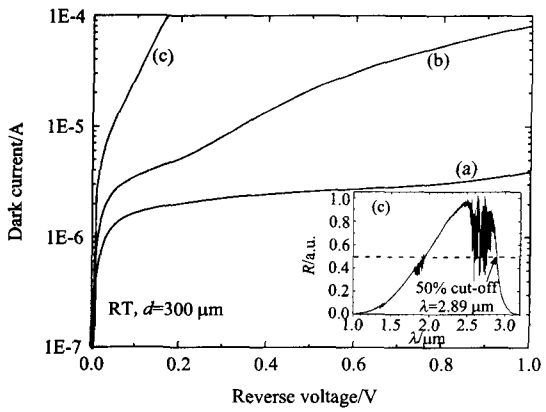

Fig. 5 *I-V* characteristics of InGaAs PDs with different lattice mismatch at room temperatures (a)1.7% (b)2.1% (c)2.6% The inset shows the response spectrum of InGaAs PD with 2.6% lattice mismatch at room temperature

图5 不同晶格失配 InGaAs 探测器的室温 *I-V* 特性 (a) 1.7% (b)2.1% (c)2.6%. 插图显示的是晶格失配度为 2.6% 的 InGaAs 探测器室温响应光谱

the InAlAs buffer layer[10]. The inset of Fig. 5 shows the response spectrum at room temperature of sample (c); the fluctuations in the response spectrum around 1.4μm, 1.9μm, and 2.5 ~ 2.8μm correspond to the water vapor absorption bands. The PD shows response peak at about 2.64μm, with 50% cut-off wavelength of 2.89μm, which matches quite well with the PL results. Therefore, for the metamorphic InGaAs PDs with lattice mismatch to the InP substrate from 1.7% to 2.6%, the grading rate of around 1% μm^{-1} should be slow enough. It is inappropriate to expect the further improvement of the PD performance by slowing the grading rate alone.

3 Conclusions

InP-based metamorphic InGaAs PD structures with lattice mismatch up to 2.6% have been grown on InAlAs continuously graded buffers with a relatively high mismatch grading rate of 1.1% μm^{-1} by GSMBE, and compared to the samples with the same structures but smaller lattice mismatch of 1.7% and 2.1% to the InP substrate. The characteristics were investigated by the measurements of AFM, x-ray diffraction, PL and device performances. Results show that the buffer layers with relatively high mismatch grading rate are efficient for the metamorphic PD structures. Moderate surface morphology, large degree of relaxation and feasible optical characteristics have been obtained. The cut-off wavelength of the device with 2.6% mismatch to the InP substrate is about 2.9μm at room temperature, while a typical dark current of 2.56μA at the reverse voltage of 10mV has been achieved for the device with 300μm diameter.

REFERENCES

[1] Kleipool Q L, Jongma R T, Gloudemans A M S, *et al.* In-flight proton-induced radiation damage to SCIAMACHY's extended-wavelength InGaAs near-infrared detectors [J]. *Infrared Phys. Technol.*, 2007, **50**(1): 30—37.

[2] Cohen M J, Olsen G H. Room-temperature InGaAs camera for NIR imaging[J]. *Proc. SPIE*, 1993, **1946**: 436—443.

[3] Wernsman B, Siergiej R R, Link S D, *et al.* Greater than 20% radiant heat conversion efficiency of a thermophotovoltaic radiator/module system using reflective spectral control [J]. *IEEE Trans. Electron Devices*, 2004, **51**(3): 512—515.

[4] Zhang Y G, Tian Z B, Zhang X J, *et al.* An innovative gas sensor with on-chip reference using monolithic twin laser [J]. *Chin. Phys. Lett.*, 2007, **24**(10): 2839—2841.

[5] Linga K R, Olsen G H, Ban V S, *et al.* Dark current analysis and characterization of $In_xGa_{1-x}As/InAs_yP_{1-y}$ graded photodiodes with $x > 0.53$ for response to longer wavelengths ($>1.7\mu m$) [J]. *IEEE J. Lightwave Technol.*, 1992, **10**(8): 1050—1055.

[6] Kim D S, Forrest S R, Lange M J, *et al.* A three wavelength infrared focal plane array detector element[J]. *IEEE Photonics Technol. Lett*, 1994, **6**(2): 235—238.

[7] D'Hondt M, Moerman I, Demeester P. Dark current optimization for MOVPE grown 2.5μm wavelength InGaAs photodetectors[J]. *Electron. Lett.*, 1998, **34**(9): 910—912.

[8] Joshi A, Becker D. High-speed low-noise p-i-n InGaAs photoreceiver at 2μm wavelength[J]. *IEEE Photonics Technol. Lett.*, 2008, **20**(8): 551—553.

[9] Zhang Y G, Gu Y, Wang K, *et al.* Properties of gas source molecular beam epitaxy grown wavelength extended InGaAs photodectector structures on linear graded InAlAs buffer [J]. *Semicon. Sci. Technol.*, 2008, **23**(12): 125029.

[10] Tian Z B, Gu Y, Wang K, *et al.* Gas source MBE-grown metamorphic InGaAs photodetectors using InAlAs buffer and cap layers with cut-off wavelength up to 2.7μm[J]. *Chin. Phys. Lett.*, 2008, **25**(6): 2292—2295.

[11] Hudait M K, Lin Y, Wilt D M, *et al.* High-quality $InAs_yP_{1-y}$ step-graded buffer by molecular beam epitaxy [J]. *Appl. Phys. Lett.*, 2003, **82**(19): 3212—3214.

[12] Fewster P F. X-ray diffraction from low-dimensional structures[J]. *Semicon. Sci. Technol.*, 1993, **8**(11): 1915—1934.

[13] Chauveau J M, Androussi Y, Lefebvre A, *et al.* Indium content measurements in metamorphic high electron mobility transistor structures by combination of x-ray reciprocal space mapping and transmission electron microscopy [J]. *J. Appl. Phys.*, 2003, **93**(7): 4219—4225.

[14] Vurgaftman I, Meyer J R, Ram-Mohan L R. Band parameters for III-V compound semiconductors and their alloys [J]. *J. Appl. Phys.*, 2001, **89**(11): 5815—5875.